



Comparison of a simple and a detailed model of magnetic hysteresis with measurements on electrical steel

Hanif Tavakoli

*School of Electrical Engineering, Royal Institute of Technology,
Stockholm, Sweden*

Dierk Bormann

ABB AB – Corporate Research, Power Technologies, Västerås, Sweden, and

David Ribbenfjärd and Göran Engdahl

*School of Electrical Engineering, Royal Institute of Technology,
Stockholm, Sweden*

Abstract

Purpose – For efficient magnetic field calculations in electrical machines, the hysteresis and losses in laminated electrical steel must be modeled in a simple and reliable way. The purpose of this paper is to investigate and discuss the potential of a simple complex-permeability model.

Design/methodology/approach – A frequency dependent complex-permeability model as well as a more detailed model (describing hysteresis, classical eddy current effects, and excess losses separately) are compared to single-sheet measurements on laminated electrical steel. It is discussed under which circumstances the simple complex- μ model is an adequate substitute for the more detailed model.

Findings – A satisfactory agreement of the simple complex- μ model was found with both detailed model and measurements, improving with increasing frequencies. This is true not only for the effective permeability function, but holds also for the detailed H - B characteristics (hysteresis).

Originality/value – It is demonstrated that the complex- μ model is a reliable and convenient starting point for the estimation of flux distribution and losses in complicated magnetic core geometries.

Keywords Electrical machines, Steel, Permeability, Eddy currents, Electromagnetism

Paper type Research paper



1. Introduction

Recent research has resulted in detailed models of the magnetic hysteresis and loss mechanisms in a wide frequency range (Bertotti, 1998; Ribbenfjärd, 2007; Ribbenfjärd and Engdahl, 2008). Although these models provide a good description of magnetic material properties or of simple reluctance circuits based on them, they are too demanding numerically to be incorporated into a full-scale magnetic field simulation of a realistic geometry, as with a FEM or FDM calculation tool. In other words, while such a detailed simulation of the H - B relation of a single or a few interacting cells is still perfectly feasible, simulating thousands or ten thousands of them simultaneously may be inconvenient or impossible.

Moreover, in many practical situations a detailed description is not required either. Often, the goal is to obtain a good estimate of some local or global quantity containing much less information than the detailed local H - B relation, such as the local losses causing dangerous hot spots, or simply the total losses in a machine relevant for cooling or economic reasons. For such applications, it is desirable to use a simple model of magnetic hysteresis and losses, which can easily be incorporated in field calculation tools but which at the same time is sufficiently close to reality, within the frequency range of interest for the specific application. Such a model is the description of magnetic (meta-)materials by a suitable frequency dependent complex permeability, which is the most general linear description of a local and isotropic H - B relation. If desired, it can easily be extended to a nonlocal and/or anisotropic H - B relation by turning μ from a scalar function of position into a distance dependent integral kernel and/or tensor, respectively, (Jackson, 1998).

In this paper, we discuss to which extent the measurement results obtained with a single-sheet tester on strips of electrical steel can reliably be described by a simple complex permeability function of frequency. Both the resulting H - B curves and the effective complex permeability are compared to the measured data at different frequencies.

For comparison, we also report simulation results obtained with a much more detailed model of the magnetic hysteresis, eddy currents and excess losses.

2. The complex-permeability model

Reduced to its simplest terms, hysteresis introduces a time phase difference between B and H . B is assumed to lag H by a constant angle θ_h called the hysteresis angle. In such a description, harmonics introduced by saturation are ignored, and the hysteresis loop becomes an ellipse whose major axis is inclined by an angle θ_h relative to the H -axis. Using complex field components \hat{B} and \hat{H} , we can define a low-frequency complex permeability including hysteresis as:

$$\hat{\mu}_h = \frac{\hat{B}}{\hat{H}} = \mu_0 \mu_r e^{-j\theta_h}. \quad (1)$$

In addition to this, eddy currents in the lamination sheets introduce frequency dependence. We briefly sketch the well-known procedure for deriving the effective frequency dependent complex permeability (Stoll, 1974). Faraday's law:

$$\nabla \times \mathbf{E} = - \frac{\partial \mathbf{B}}{\partial t} \quad (2)$$

and Ampere's law:

$$\nabla \times \mathbf{H} = \mathbf{J} + \frac{\partial \mathbf{D}}{\partial t}, \quad (3)$$

in combination with the constitutive relations:

$$\mathbf{J} = \sigma \mathbf{E}, \quad \mathbf{D} = \varepsilon \mathbf{E}, \quad \mathbf{B} = \hat{\mu}_h \mathbf{H}, \quad (4)$$

and time-harmonic assumption lead to:

$$\nabla^2 \mathbf{H} = \hat{\alpha}^2 \mathbf{H} = j\omega \hat{\mu}_h (\sigma + j\omega \varepsilon) \mathbf{H}. \quad (5)$$

For lower frequencies when wave propagation can be ignored (i.e. $\sigma \gg \omega\epsilon$), we have $\hat{\alpha}^2 \approx j\omega\hat{\mu}_h\sigma$.

For analysis of the magnetic field in a laminate, the simple geometry shown in Figure 1 is appropriate. The magnetic field is applied in the z -direction, hence the only component of the magnetic field strength is H_z which varies only in the x -direction, $H_z = H_z(x)$. In one dimension, equation (5) reduces to:

$$\frac{\partial^2 H_z}{\partial x^2} = \hat{\alpha}^2 H_z, \quad (6)$$

which has the general solution:

$$H_z(x) = A_1 e^{\hat{\alpha}x} + A_2 e^{-\hat{\alpha}x}. \quad (7)$$

The field strength on the both sides of the laminate is assumed to be H_0 . For the reason of symmetry, the following condition is obtained:

$$H_z(b) = H_z(-b) = H_0. \quad (8)$$

The final expression for the magnetic field strength then becomes:

$$H_z(x) = H_0 \frac{\cosh(\hat{\alpha}x)}{\cosh(\hat{\alpha}b)}. \quad (9)$$

The effective, complex permeability of a lamination is given as the average magnetic flux density \bar{B} in the laminate normalized to the surface magnetic field strength H_0 :

$$\hat{\mu}_{\text{eff}} = \mu'_{\text{eff}} - j\mu''_{\text{eff}} = \frac{\bar{B}}{H_0} = \frac{1}{H_0 2b} \int_{-b}^b \hat{\mu}_h H_z(x) dx = \hat{\mu}_h \frac{\tanh(\hat{\alpha}b)}{\hat{\alpha}b}. \quad (10)$$

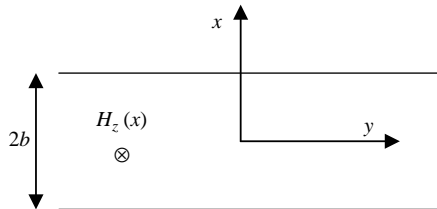
This expression accounts for the effect of hysteresis without saturation, and the effect of eddy currents. We assume here that additional (or “excess”) losses are either negligible or have a similar frequency dependence so that they can be incorporated in the expression (10) for $\hat{\mu}_{\text{eff}}$.

3. The detailed hysteresis model

Later in this paper, we will report some results obtained with a more detailed model of the magnetic hysteresis, eddy current and excess losses, which is therefore described here in some detail.

The total hysteresis is a combination of three different phenomena, namely, static hysteresis, eddy current effects and excess eddy currents. For the detailed hysteresis model, the following approach has been used. The static hysteresis is modeled using

Figure 1.
Laminate infinite in z direction, with a width in y direction much larger than its thickness $2b$, exposed to a H field in z direction



Bergqvist's (1994, 1997) lag model, the classical eddy currents are modeled using Caer circuits (de León and Semlyen, 1994; Ribbenfjärd and Engdahl, 2008), and the excess losses are modeled using an approach by Bertotti (1998).

3.1 Static hysteresis

The lag model of static hysteresis starts from the idea that the magnetic material consists of a finite number of pseudo-particles, i.e. volume fractions with different magnetization. The total magnetization is then a weighted sum of the individual magnetization of all pseudo-particles.

The hysteresis curve for one particle is introduced by applying a “play operator” with “pinning strength” k (which will determine the width of the hysteresis curve) on the anhysteretic curve (Figure 2).

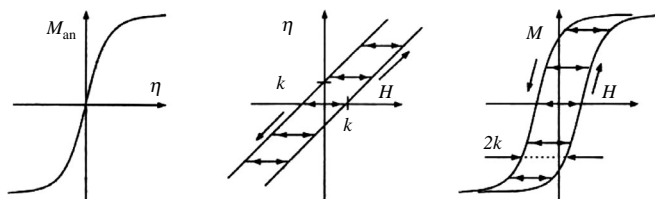
Using a population of pseudo-particles with different pinning strengths allows to construct minor loops. We assign an individual pinning strength $\lambda_i k$ to every pseudo-particle, where k is the mean pinning strength, and the λ_i are dimensionless numbers. The total magnetization is then given by a weighted superposition of the contributions from all pseudo-particles (Figure 3). The expression:

$$M_{\text{an}}(H) = \frac{2}{\pi} M_s \arctan\left(\frac{\pi H \chi}{2M_s}\right) \quad (11)$$

is used for the anhysteretic magnetization, where M_s is the saturation magnetization and χ is the susceptibility at $H = 0$. The total magnetization of the material is then given by:

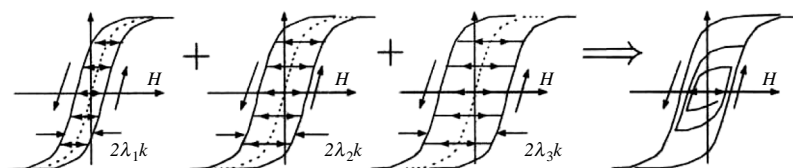
$$M = cM_{\text{an}}(H) + \int_0^\infty M_{\text{an}}(P_{\lambda k}(H)) \zeta(\lambda) d\lambda, \quad (12)$$

where c is a constant that governs the degree of reversibility, and the integral describes the hysteretic behavior (irreversible part). $P_{\lambda k}$ is a play-operator with the pinning strength λk , and $\zeta(\lambda)$ is a weight function describing the density of the pseudo-particles. Finally, the magnetic flux density is obtained from $B = \mu_0(H + M)$.



Source: Ribbenfjärd (2007)

Figure 2. Anhysteretic curve (left), play operator (middle), and resulting hysteresis curve (right)



Source: Ribbenfjärd (2007)

Figure 3. Weighted superposition of the contributions from pseudo-particles describes a minor loop

3.2 Excess losses

Excess losses are caused by microscopic eddy currents induced by local changes in flux density due to domain wall movements. For our detailed model, we use an approach described by Bertotti (1998). In this approach, a number of active correlation regions are assumed randomly distributed in the material. The correlation regions are connected to the micro-structure of the material like grain size, crystallographic textures and residual stresses. In Bertotti's model, the resulting contribution to the magnetic field strength is given by:

$$H_{\text{excess}} = \frac{n_0 V_0}{2} \left(\sqrt{1 + \frac{4\sigma G 2bw}{n_0^2 V_0} \left| \frac{dB}{dt} \right|} - 1 \right) \text{sign} \left(\frac{dB}{dt} \right), \quad (13)$$

where w is the width of the laminate and $2b$, as before, its thickness. G is a parameter depending on the structure of the magnetic domains. n_0 is a phenomenological parameter related to the number of active correlation regions when the frequency approaches zero, whereas V_0 determines to which extent micro-structural features affect the number of active correlation regions.

The parameters n_0 and V_0 are by definition frequency independent, but they are expected in reality to depend on the amplitude of the B field (Barbisio *et al.*, 2004). Since the precise form of this dependence is unknown, their values are usually adjusted empirically for given amplitude. In the simulations reported here we use one set of (empirically determined) values, although the amplitude of the B field slightly varies in the measurements.

4. The measurement setup

The magnetic measurements were carried out using a single-sheet tester. It consists of two equal U-shaped yokes placed face-to-face to each other (Figure 4). The magnetic sheet to be tested is placed between the yokes and most of the flux is forced through it due to its high permeability. For the measurement of the flux in the test material, a coil is surrounding the strip which is connected to a flux meter. The magnetic field strength

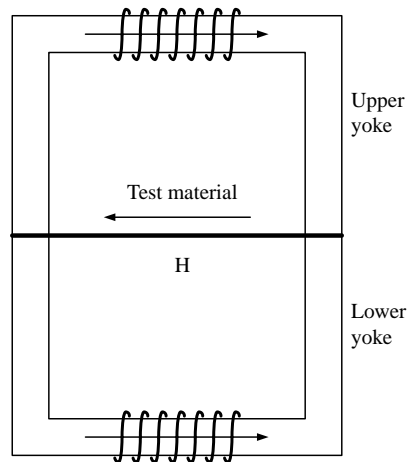


Figure 4.
Schematic view of our
single-sheet tester

is measured with a Hall probe placed close to the surface of the sample and connected to a Tesla meter. A sinusoidal H field was applied to the sample; the H and B field values were measured for 100 periods and numerically filtered. Thereafter, the mean values at different phase angles of the B and H fields were calculated. These values were then used in the paper.

We approximate the measured H - B curve with a complex- μ ellipse characterized by the permeability $\hat{\mu}_{\text{meas}}$ by matching both its peak values H_p , B_p and its area A to the measured results. This is, of course, appropriate as long as the shape of the measured H - B curve is close to an ellipse, i.e. if saturation effects are not too pronounced. The area A , which measures the power loss per cycle, is given by the integral:

$$A = \oint B_{\text{meas}} dH_{\text{meas}} = \int_0^T B_{\text{meas}} \frac{dH_{\text{meas}}}{dt} dt, \quad (14)$$

where B_{meas} and H_{meas} are the time dependent measured B and H fields, respectively, and T is the duration of a period. If the measured magnetic field strength is assumed to vary sinusoidally:

$$H_{\text{meas}}(t) = \text{Re} (H_p e^{j\omega t}) = H_p \cos(\omega t), \quad (15)$$

then its derivative becomes:

$$\frac{dH_{\text{meas}}(t)}{dt} = -\omega H_p \sin(\omega t), \quad (16)$$

and the measured magnetic flux density:

$$\begin{aligned} B_{\text{meas}}(t) &= \text{Re} (\hat{\mu}_{\text{meas}} H_p e^{j\omega t}) \\ &= \text{Re} ((\mu'_{\text{meas}} - j\mu''_{\text{meas}}) H_p e^{j\omega t}) \\ &= H_p (\mu'_{\text{meas}} \cos(\omega t) + \mu''_{\text{meas}} \sin(\omega t)). \end{aligned} \quad (17)$$

By inserting equations (15) and (16) into equation (14), we get:

$$\mu''_{\text{meas}} = -\frac{A}{\pi H_p^2}. \quad (18)$$

Furthermore, from the relation $|\hat{\mu}_{\text{meas}}| H_p = B_p$, we obtain:

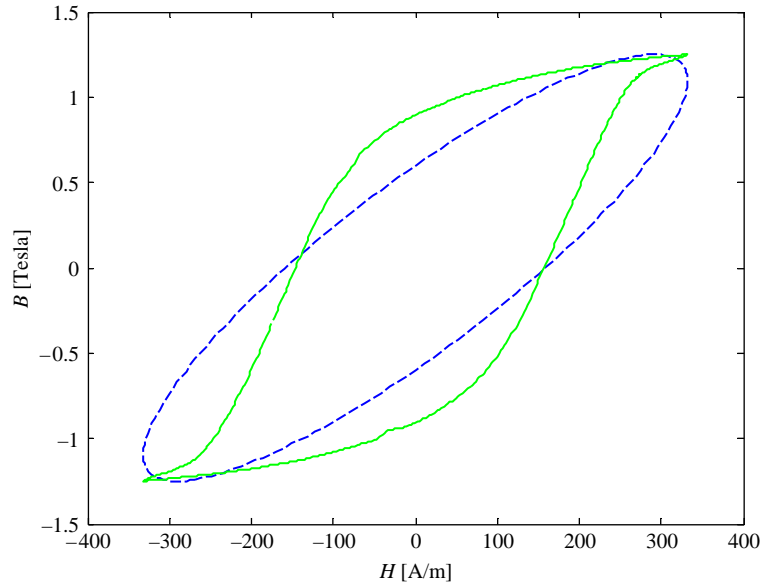
$$|\hat{\mu}_{\text{meas}}|^2 = (\mu'_{\text{meas}})^2 + (\mu''_{\text{meas}})^2 = \left(\frac{B_p}{H_p} \right)^2, \quad (19)$$

which implies:

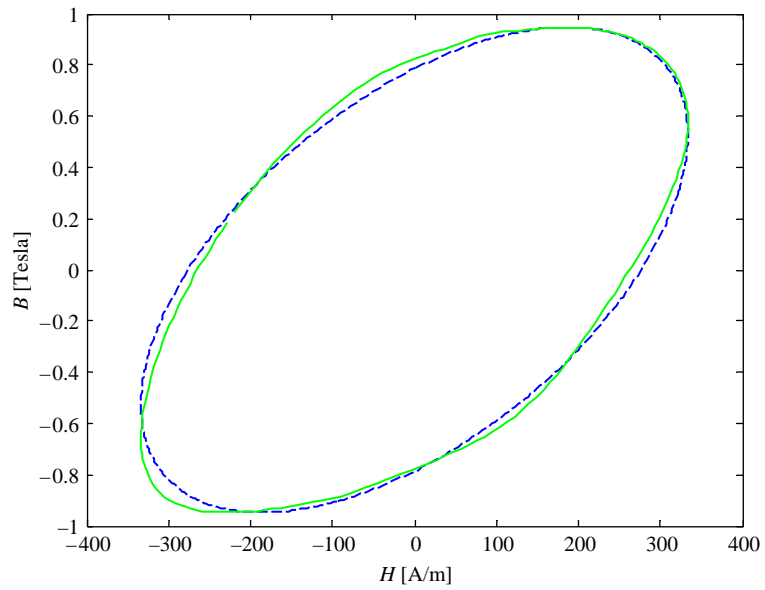
$$\mu'_{\text{meas}} = \sqrt{\left(\frac{B_p}{H_p} \right)^2 - (\mu''_{\text{meas}})^2}. \quad (20)$$

Both μ'_{meas} and μ''_{meas} are functions of frequency.

Figure 5 compares the measured H - B curves with complex- μ ellipses, generated with the adapted $\hat{\mu}_{\text{meas}}$ at frequencies $f = 50$ and 400 Hz.



(a)



(b)

Figure 5.
H-B-curves from
measurements (solid gray
line) and complex- μ model
(dashed line) with
 $\hat{\mu}_{\text{meas}} = \mu'_{\text{meas}} - j\mu''_{\text{meas}}$,
for (a) $f = 50$ Hz and
(b) $f = 400$ Hz

$\hat{\mu}_{\text{eff}}$ as defined in equation (10) is a function of frequency and of a vector $\mathbf{x} = (\mu_r, \theta_h, \sigma b^2)$ containing the model parameters. It is adjusted to the measured data by numerically minimizing the expression:

$$\sum_{i=1}^N |\hat{\mu}_{\text{eff}}(\mathbf{x}, \omega_i) - \hat{\mu}_{\text{meas}}(\omega_i)|^2 \quad (21)$$

with respect to \mathbf{x} . $\hat{\mu}_{\text{meas}}(\omega_i)$ are the measured complex permeability values, defined by equations (18) and (20), at N different frequencies $\omega_i = 2\pi f_i$, $i = 1, \dots, N$. We performed measurements at $N = 9$ different frequencies ranging from 50 Hz to 2 kHz (Figures 6 and 7), on a 100 mm \times 3.2 mm strip of the non-oriented magnetic material M600 with a thickness of $2b = 0.5$ mm.

5. Results and discussion

Since the measurement setup was quite sensitive to noise, the measurements had to be numerically filtered. Adjusting $\hat{\mu}_{\text{eff}}$ to the filtered data using equation (21), we obtain the following model parameter values: $\mu_r = 3366$; $\theta_h = 0.477$ rad; and $\sigma b^2 = 0.243$ Sm, i.e. $\sigma = 3.89 \times 10^6$ S/m. The last value is somewhat larger than the true dc conductivity of this material, $\sigma_{\text{dc}} = 3.33 \times 10^6$ S/m, since we have included here excess losses in the classical phenomenological form (equation (10)).

In Figure 6, the real and imaginary parts of the measured complex permeability are compared at different frequencies with the adjusted $\hat{\mu}_{\text{eff}}$. The agreement is quite satisfactory considering the simplicity of the model, especially at higher frequencies.

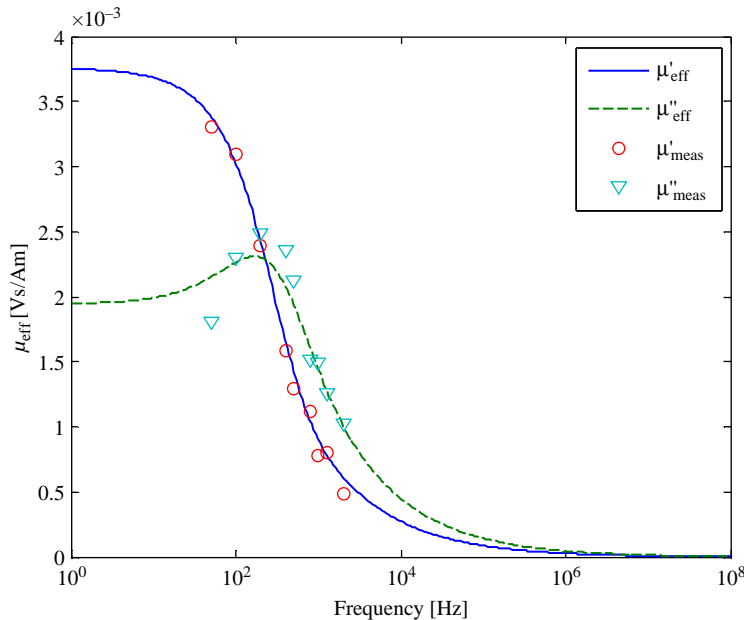


Figure 6. Real and imaginary parts of the measured complex permeability μ_{meas} (symbols) and of the fitted permeability function μ_{eff} (curves)

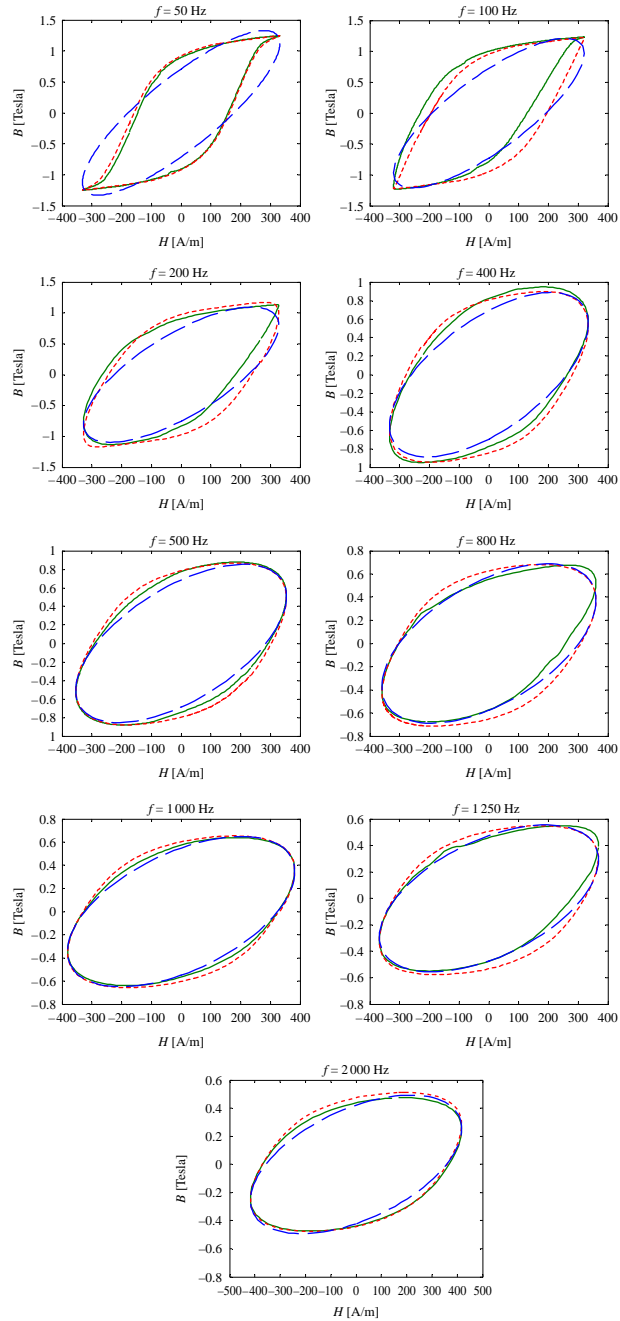


Figure 7.
 H - B curves from measurements (solid gray line), detailed model (dotted line) and complex- μ model (dashed line) with μ calculated from expression (10), at different frequencies ranging from 50 Hz to 2 kHz

The deviation between μ''_{meas} and μ''_{eff} at the lowest frequency is probably due to saturation effects which are not properly taken into account by the expression (10) for μ_{eff} , see for instance the measurement at 50 Hz (Figure 5(a)). The amplitude had to be chosen large enough for the signal not to be covered by noise.

The above way of defining a “best fit” of ellipses to the more complicated H - B hysteresis relations approximately preserves both H and B amplitudes and magnetic losses in the whole frequency range. This is shown in the Figure 7, where the measured H - B curves are compared with the corresponding complex- μ ellipses and the detailed model at all measured frequencies. As can be seen, the simple model agrees very well with the measurements as long as saturation is not too strong, which means for low-amplitude fields and/or for frequencies higher than about 200 Hz.

6. Conclusions

In this paper, a simple, frequency dependent complex- μ model of magnetic core material has been developed and adjusted to measurements. Its real and imaginary parts were compared to measurements in a wide frequency range. The agreement was found satisfactory, especially for higher frequencies, which makes the complex- μ model a very convenient starting point for the estimation of flux distribution and losses in complicated core geometries.

Furthermore, H - B curves from our measurements, the simple complex- μ model and the detailed hysteresis model were compared for different frequencies. Again, the results from the complex- μ model were found to agree well with measurements at higher frequencies. At low-frequencies and high-field amplitudes the complex- μ model deviates from measurements and detailed hysteresis model, since it does not take saturation effects properly into account. This is, however, not expected to affect its usefulness for loss estimation.

References

- Barbaisio, E., Fiorillo, F. and Ragusa, C. (2004), “Predicting loss in magnetic steels under arbitrary induction waveform and with minor hysteresis loops”, *IEEE Transactions on Magnetics*, Vol. 40 No. 4, pp. 1810-9.
- Bergqvist, A. (1994), “A phenomenological differential-relation-based vector hysteresis model”, *Journal of Applied Physics*, Vol. 75 No. 10, pp. 5484-6.
- Bergqvist, A. (1997), “Magnetic vector hysteresis model with dry friction-like pinning”, *Physica B: Condensed Matter*, Vol. 233 No. 4, pp. 342-7.
- Bertotti, G. (1998), *Hysteresis in Magnetism*, Academic Press, San Diego, CA.
- de León, F. and Semlyen, A. (1994), “Complete transformer model for electromagnetic transients”, *IEEE Transactions on Power Delivery*, Vol. 9 No. 1, pp. 231-9.
- Jackson, J.D. (1998), *Classical Electrodynamics*, 3rd ed., Wiley, New York, NY.
- Ribbenfjärd, D. (2007), “A lumped transformer model including core losses and winding impedances”, Licentiate thesis in Electromagnetic Engineering, Royal Institute of Technology, Stockholm.
- Ribbenfjärd, D. and Engdahl, G. (2008), “Novel method for modelling of dynamic hysteresis”, *IEEE Transactions on Magnetics*, Vol. 44 No. 6, pp. 854-7.
- Stoll, R.L. (1974), *The Analysis of Eddy Currents*, Clarendon Press, Oxford.

About the authors



Hanif Tavakoli received the Master degree in Electrical Engineering from the Royal Institute of Technology (KTH) in Stockholm, Sweden, in 2006. Currently, he works towards a PhD degree in Electro Technical Modeling and Construction in the School of Electrical Engineering at KTH. His research is on electromagnetic modeling of transformers, and frequency response analysis modeling and measurements for transformer windings.



Dierk Bormann holds a PhD in Physics (1992) from the University of Heidelberg (Germany). After some years of academic research in the fields of statistical physics, low-dimensional quantum systems, superconductivity and superfluidity, he joined ABB Corporate Research (Västerås, Sweden) in 2000. His current research interests include transient modeling of electrical apparatus and machines, electrical breakdown, and arc physics. He is a member of the American and German Physical Societies and has served since several years in a Working Group of the Cigré SC A2 (Transformers). Dierk Bormann is the corresponding author and can be contacted at: dierk.bormann@se.abb.com



David Ribbenfjärd is currently PhD student at the Royal Institute of Technology, Stockholm, Sweden. David also holds a Tech. Lic. in Electrical Power Systems (2007) from the same university. His research mainly concerns electromagnetic modeling of power transformers.



Göran Engdahl, senior member of IEEE, was born in Uppsala, Sweden in 1948. He received his Master of Science degree in Electro Physics at Uppsala University in 1974 and his PhD degree in Electricity from the Faculty of Natural Science, Uppsala University in 1981. He has been working as First Research Engineer at National Road and Traffic Research Institute, Linköping, First Researcher at Swedish Defence Research Agency, Linköping – 1983, Research Engineer at ABB Corporate Research 1983-2001, and Associate Professor at the Royal Institute of Technology 1996-2001. Since 2001, he works as a Professor at the School of Electrical Engineering at the Royal Institute of Technology. One topic he is interested in is modeling and design of electrical apparatus and systems comprising magnetic materials and he is the author of more than 80 publications.